INTERPRETATION OF NUMERICAL TRANSPORT EXPERIMENTS IN ALLUVIAL SEDIMENTS WITH SINGLE–DOMAIN, DUAL–POROSITY AND DUAL–PERMEABILITY MODELS

F. Baratelli, L. Cattaneo, C. Vassena, M. Giudici, G. Parravicini

Università degli Studi di Milano, Dipartimento di Scienze della Terra "A. Desio", Sez. di Geofisica, via Cicognara 7, 20129 Milano, Italy

Università degli Studi di Milano, Dipartimento di Fisica, via Celoria 16, 20133 Milano, Italy

fulvia.baratelli@unimi.it

Motivations:

• Alluvial aquifers are characterized by **heterogeneity** of the sediments at the **fine scale**, which significantly affects groundwater flow and solute transport at the **macroscopic scale**, that is of interest for practical applications.

• The spatio-temporal evolution of a solute's plume released in an aquifer strongly depends on the hydrofacies **connectivity**, which controls the existence of **preferential flow paths** (PFPs) or **hydraulic barriers**.

• The classical **single-domain approach** cannot describe the effects of heterogeneity and can lead to the underestimation of the travel times of the particles of solute, which might be a serious issue for practical applications, as the studies of groundwater contamination by pollutants.

• The objective of this work is to test the performance of different transport models (**single and dual-domain models**) for the interpretation of some numerical transport experiments of a conservative solute in a heterogeneous domain.

Case study:

Three prismatic blocks of sediments (volume ≈ 3 m^3) dug at a quarry site into natural sediments belonging to the Pleistocene sequences of the Ticino basin (Northern Italy).

• Geological and hydrostratigraphical model

• 3D geostatistical simulation (five operative facies)

Numerical tracer tests:

A numerical experiment is performed to simulate the **instantaneous injection** of a mass of a conservative solute through the upstream face of the block.

• the **flow field** is simulated with a flow model for steady state saturated flow, with the following boundary conditions:

  ◦ constant heads on the two faces perpendicular to the flow direction (unit hydraulic gradient);

  ◦ no flow along faces parallel to the flow direction.

• convective transport modelled with a **particle tracking** technique

• virtual field data: arrival time of the particles at the downstream face of the block → **'experimental' cumulative breakthrough curve** (cumulative BTC)

Model block 1 (MB1)

dug into a sand dune, which develops above a gravel/sand cross-laminated bar unit

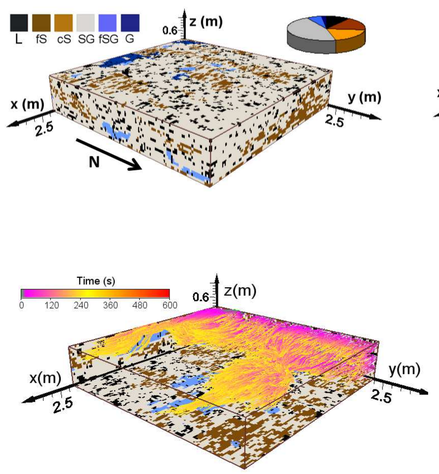

Model block 2 (MB2)

dug into a cross-stratified gravel/sand bar, with patches of open framework clean gravel

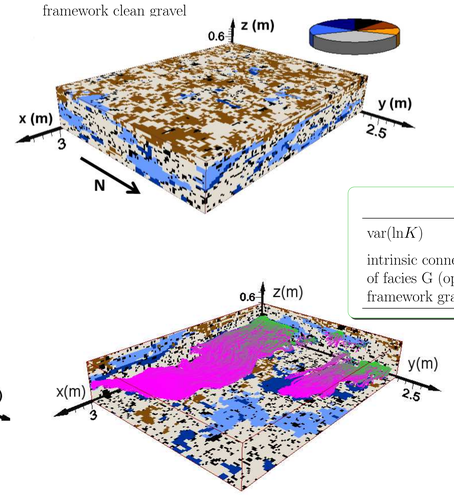

Model block 3 (MB3)

dug from mostly disorganized gravel-sands that cover a gravel-sand unit

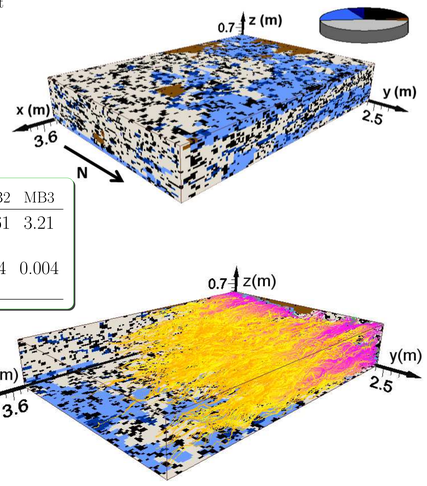

	MB1	MB2	MB3
var($\ln K$)	1.52	3.61	3.21
intrinsic connectivity of facies G (open framework gravel)	0.3	0.4	0.004

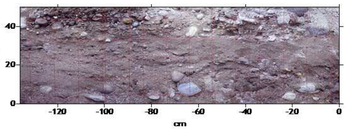

Single-domain

Dual-porosity

Uncoupled dual-permeability

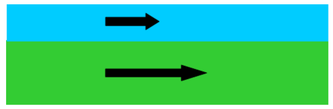

Coupled dual-permeability

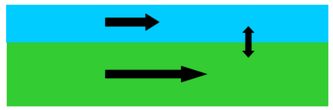

Transport models:

(1) Single–domain model:

It consists of the classical advective–dispersive equation (**ADE**):

$$\frac{\partial C}{\partial t} = -v\frac{\partial C}{\partial x} + D\frac{\partial^2 C}{\partial x^2}$$

(2) Dual–domain models: the heterogeneous porous medium is modelled as a superposition of two domains with different transport properties

(2.1) Dual–porosity model: water can flow in one of the two domains (**mobile domain**) but not in the other (**immobile domain**) and the two domains can exchange solute.

$$\frac{\partial C^{\mathrm{mob}}}{\partial t} = -v\frac{\partial C^{\mathrm{mob}}}{\partial x} + D\frac{\partial^2 C}{\partial x^2} - \frac{\alpha}{n^{\mathrm{mob}}}\left(C^{\mathrm{mob}} - C^{\mathrm{im}}\right)$$
$$\frac{\partial C^{\mathrm{im}}}{\partial t} = \frac{\alpha}{n^{\mathrm{im}}}\left(C^{\mathrm{mob}} - C^{\mathrm{im}}\right)$$

(2.2) Dual–permeability models: water can flow with different velocities in the two domains: a **fast domain** (H) and a **slow domain** (L), characterized by higher and lower hydraulic conductivities respectively.

$$\frac{\partial C^{(\mathrm{H})}}{\partial t} = -v^{(\mathrm{H})}\frac{\partial C^{(\mathrm{H})}}{\partial x} + D^{(\mathrm{H})}\frac{\partial^2 C}{\partial x^2} - \frac{\alpha}{\varepsilon^{(\mathrm{H})}n^{(\mathrm{H})}}\left(C^{(\mathrm{H})} - C^{(\mathrm{L})}\right)$$
$$\frac{\partial C^{(\mathrm{L})}}{\partial t} = -v^{(\mathrm{L})}\frac{\partial C^{(\mathrm{L})}}{\partial x} + D^{(\mathrm{L})}\frac{\partial^2 C}{\partial x^2} + \frac{\alpha}{\varepsilon^{(\mathrm{L})}n^{(\mathrm{L})}}\left(C^{(\mathrm{H})} - C^{(\mathrm{L})}\right)$$

(2.2.1) Uncoupled: the two domains do not exchange solute ($\alpha = 0$).
(2.2.2) Coupled: the two domains can exchange solute ($\alpha \neq 0$).

Notation

C	concentration	$v^{(H)}$, $v^{(L)}$	mean pore water velocity in the (H) and (L) domains
v	mean pore water velocity	$D^{(H)}$, $D^{(L)}$	longitudinal component of the dispersion tensor in the (H) and (L) domains
D	longitudinal component of the dispersion tensor	$\varepsilon^{(H)}$, $\varepsilon^{(L)}$	fraction of the total volume occupied by the (H) and (L) domains
C^{mob}, C^{im}	concentration in the mobile and immobile domains	$n^{(H)}$, $n^{(L)}$	porosity of the (H) and (L) domains
n^{mob}, n^{im}	porosity of the mobile and immobile domains	q_c	solute flux (BTC)
α	solute exchange coefficient	$\mathcal{M}$	cumulative solute flux (cumulative BTC)
$C^{(H)}$, $C^{(L)}$	concentration in the fast (H) and slow (L) domains	$\mathcal{M}^{(H)}$, $\mathcal{M}^{(L)}$	cumulative solute flux in the (H) and (L) domains
		K	hydraulic conductivity

References:

• Zappa et al. (2006), *J Hydrol*, **325**, 134-153.

• Vassena et al. (2010), *Hydrogeol J*, **18**, 651-668.

• Baratelli et al. (2011), *Transport Porous Med*, **87(2)**, 465-484.

Initial and boundary conditions:

Initially there is no solute in the domain, and at time $t = 0$ a mass M of solute per unit surface of the block is **injected instantaneously** in $x = 0$; for the single-domain model:

I.C. $C(x,0) = 0,\ x > 0$

B.C. $q_c(0,t) = M\delta(t),\ t \geq 0$
$\lim_{x\to+\infty} C(x,t) = 0,\ t \geq 0$

where q_c denotes the BTC, i.e., the mass of solute that crosses the unit surface in the unit time.

These conditions are easily generalized to the other transport models. Notice that in the case of the dual-porosity model, all the solute mass is injected into the mobile domain, whereas in the case of the dual-permeability models, the solute mass injected is subdivided among the two domains, according to the following relation: $M = \varepsilon^{(H)}M^{(H)} + \varepsilon^{(L)}M^{(L)}$.

Solution of the equations:

► The single-domain and uncoupled dual-permeability models can be solved *analytically* for the cumulative BTC $\mathcal{M}$:

Single-domain model:

$$\mathcal{M}(x,t) = \frac{Mx}{\sqrt{4\pi D}}\int_0^t t'^{-3/2}\exp\left[-\frac{(x-vt')^2}{4Dt'}\right]dt' \qquad (1)$$

Uncoupled dual-permeability model:

$$\mathcal{M}(x,t) = \varepsilon^{(H)}\mathcal{M}^{(H)}(x,t) + \varepsilon^{(L)}\mathcal{M}^{(L)}(x,t), \qquad (2)$$

where $\mathcal{M}^{(H)}$ and $\mathcal{M}^{(L)}$ are given by (1), after substituting the parameters of the corresponding domains.

► A *numerical* model is implemented for the **dual-porosity** and **coupled dual-permeability models:**

• finite differences, Crank-Nicholson

• up-wind technique for the convective term

• second-order correction to reduce numerical dispersion due to truncation errors

Calibration:

• **objective function**: mean of the squared differences between the experimental and the modeled cumulative BTC

• **Levenberg-Marquardt** algorithm

Results:

Experimental (histogram) and modeled (lines) BTCs:

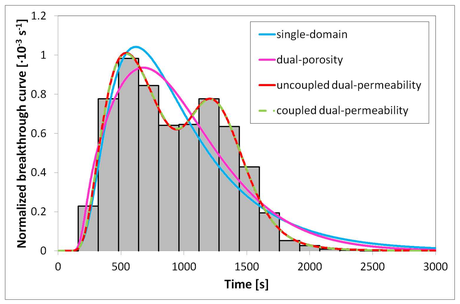

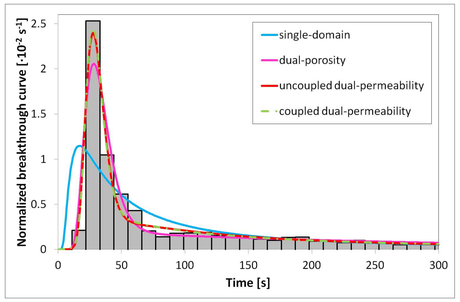

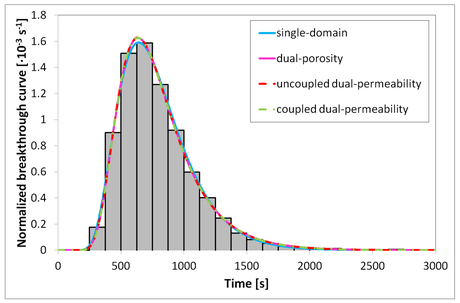

Single-domain

	D[m^2 s^{-1}]	v[m s^{-1}]
MB1	$9.05\cdot10^{-4}$	$2.45\cdot10^{-3}$
MB2	$8.90\cdot10^{-2}$	$1.47\cdot10^{-2}$
MB3	$1.07\cdot10^{-3}$	$4.44\cdot10^{-3}$

Dual-porosity

	D[m^2 s^{-1}]	v[m s^{-1}]	n^{mob}	α[s^{-1}]
MB1	$5.39\cdot10^{-4}$	$7.04\cdot10^{-3}$	$7.15\cdot10^{-2}$	$9.12\cdot10^{-4}$
MB2	$1.52\cdot10^{-2}$	$8.45\cdot10^{-2}$	$4.20\cdot10^{-2}$	$8.90\cdot10^{-4}$
MB3	$9.46\cdot10^{-4}$	$4.70\cdot10^{-3}$	$1.87\cdot10^{-1}$	$6.10\cdot10^{-5}$

Uncoupled dual-permeability

	$D^{(H)}$[m^2 s^{-1}]	$D^{(L)}$[m^2 s^{-1}]	$v^{(H)}$[m s^{-1}]	$v^{(L)}$[m s^{-1}]	$\varepsilon^{(H)}$	$M^{(H)}$[kg m^{-2}]
MB1	$8.49\cdot10^{-4}$	$5.83\cdot10^{-5}$	$3.15\cdot10^{-3}$	$1.81\cdot10^{-3}$		$1.96\cdot10^{3}$
MB2	$9.60\cdot10^{-3}$	$2.95\cdot10^{-2}$	$1.00\cdot10^{-1}$	$9.34\cdot10^{-3}$		$1.04\cdot10^{3}$
MB3	$9.45\cdot10^{-4}$	$9.65\cdot10^{-4}$	$4.94\cdot10^{-3}$	$3.79\cdot10^{-3}$		$2.15\cdot10^{3}$

Coupled dual-permeability

	$D^{(H)}$[m^2 s^{-1}]	$D^{(L)}$[m^2 s^{-1}]	$v^{(H)}$[m s^{-1}]	$v^{(L)}$[m s^{-1}]	$\varepsilon^{(H)}$	$M^{(H)}$[kg m^{-2}]	α[s^{-1}]
MB1	$8.41\cdot10^{-4}$	$5.66\cdot10^{-5}$	$3.18\cdot10^{-3}$	$1.80\cdot10^{-3}$	$2.91\cdot10^{-1}$	$6.77\cdot10^{3}$	$4.65\cdot10^{-6}$
MB2	$8.62\cdot10^{-3}$	$3.79\cdot10^{-2}$	$9.84\cdot10^{-2}$	$6.00\cdot10^{-11}$	$1.96\cdot10^{-1}$	$7.50\cdot10^{3}$	$6.27\cdot10^{-4}$
MB3	$9.25\cdot10^{-4}$	$1.16\cdot10^{-3}$	$4.75\cdot10^{-3}$	$3.17\cdot10^{-3}$	$7.22\cdot10^{-1}$	$4.99\cdot10^{3}$	$1.30\cdot10^{-4}$

MB1:

• the **double peak** of the experimental BTC, which is a typical effect of the PFPs, is described by the dual-permeability models; this is not the case for the single-domain and dual-porosity models;

• the introduction of the exchange term between the two domains for the dual-permeability approach does not improve the fit of the data.

MB2:

• the three dual-domain approaches describe well the experimental BTC, by taking into account both the fast particles, corrisponding to the **early peak**, and the slow particles, that give rise to the **long tail**;

• no significant improvement from the uncoupled to the coupled dual-permeability model.

MB3:

• the experimental BTC **does not show any typical effect of the PFPs**: the data are well described already by the single-domain model.

► Relative improvement of the objective function with respect to the single-domain model (%):

	MB1	MB2	MB3
Dual-porosity	24	63	43
Uncoupled dual-permeability	82	72	43
Coupled dual-permeability	82	74	43